Joint analysis of galaxy redshift surveys and Lyα forests I: the large-scale gasenous environment of Lyα galaxies with redshift-space distortion

Koki Kakiichi et al,[1][*]

[1] *Max Planck Institute for Astrophysics, Karl-Schwarzschild Straße 1, 85741 Garching, Germany*

Released 2002 Xxxxx XX

ABSTRACT

Redshift surveys of Lyα forests and Lyα-emitting/absorbing galaxies.

Key words: atomic processes – cosmology: theory – line: formation – radiative transfer – infrared: general – scattering

1 INTRODUCTION

We propose and the explore the potentials of deep redshift surveys of Lyα galaxies in the fored gound of QSOs covering redshifts $2 < z < 8$. Joint analysis of Lyα forests and Lyα-emitting and absorbing galaxies over redshift $3 < z < 8$ enables us to investigate the Epoch of Reionization and the transition to post-reionization era, allowing to break the multiple degeneracies arising from analysis of high-redshift Lyα galaxies alone. For both Lyman-break and narrow-band selection technique, Lyα line can appear in galaxies both as emission or absorption.

The gasenous environment of galaxies is a natural consequence arising from the concordance hierarchical structure formation in ΛCDM cosmology, forming cosmic web. One effect of gasenous environment on galaxies is the impact on their formation and evolution (Dekel+), for example, the popular cold stream picture in the formation of galaxies to name a few. Another important impact of the environment is to induce the selection bias on the observation of galaxies. Since we see galaxies through their gasenous environments, any absorption or reprocessing of the light along a line of sight introduces the environmentally-induced selection bias upon observations of galaxies. One notable example of such selection bias is on the population of Lyα-emitting galaxies, which has been used to constrain the neutral fraction of the universe during the EoR. Furthermore, even at the post-reionized universe, the possibile impact on LAEs clustering due to the Lyα RT through the gasenous environment as CGM and IGM (Zheng+; Wyithe & Dijkstra; Breg+) calls for the close examination and testing this hypothesis based on observations. The degree of the environmetal impact on the LAE selection influences the interprelation of redshift BAO survey such as HETDEX to do cosmology (Wyithe&Dijkstra, Breg+).

[*] E-mail: kakiichi@mpa-garching.mpg.de

The galaxy redshift survey in the foreground of QSOs is not a new idea, which has been conducted by Aldelberger+, Cooke+, Keck Baryonic Structure Survey (KBSS, Steidel+) for $z \sim 2-3$. Yet, the connection to EoR and RT studies of galaxies and the IGM are not or only weakly made. The idea to perform the joint analysis of Lyα galaxies and QSO spectra occasionally has appeared in the literature (Baek, Ferrara & Semelin 2012, SDSS J1335+3533 good candidate?). Yet, the full potential of such survey strategy and the requirement still must be worked out. An idea is to extend such survey strategy to higher redshifts, which enable us the joint analysis of LLS/DLA, Lyα forests and galaxies for both Lyα in emission and absorption.

2 SURVEY REQUIREMENTS

We propose the sketch of survey requirement to characterise the IGM/CGM environment of Lyα-galaxies for $2 < z < 8$.

2.1 QSO fields

Firstly, the selection of the potential target fields is listed in Table 1. The redshift range covered by the Lyα forest between Lyα and Lyβ lines in the restframe of a background QSO at redshift z_Q is $\Delta z/(1+z_Q) = \Delta\lambda/\lambda_\alpha$ where $\Delta\lambda = \lambda_\alpha - \lambda_\beta$ is the wavelength interval between Lyα and Lyβ lines.

To perform the Voigt profile decomposition of Lyα forests, both high signal-to-noise ratio per pixel and high resolution (FWHM $\lesssim$ 25km/s) spectroscopy of a QSO should be obtained (Rauch 1998). For example, KBSS survey (Rudie et al. 2012) has observed 15 QSOs with Keck-/HIRES, obtaining $R \simeq 45000$ (FWHM$\simeq$ 7km/s) and S/N $\sim 50 - 200$pixel^{-1}. The resolved FWHM sets the lower limit of b-parameter can be measured from voigt profile decomposition.

Table 1. List of potential targets of QSO fields. QSOs used in Fan+2006 and Becker+2014 are listed.

QSO name	QSO redshift	
z > 6		
SDSS J1148+5251	6.4189	Fan+06
SDSS J1030+0524	6.3110	Fan+06
CFHQS J0050+3445	6.25	
SDSS J1623+3112	6.2470	Fan+06
SDSS J1048+4637	6.2284	Fan+06
SDSS J125051.93+313021.9	6.1300	Fan+06
ULAS J1319+0950	6.13	
SDSS J23150023	6.12	
SDSS J1602+4228	6.0700	Fan+06
SDSS J1630+4012	6.0650	Fan+06
SDSS J20540005	6.06	
SDSS J0353+0104	6.05	
SDSS J0818+1722	6.02	Fan+06
SDSS J1306+0356	6.0160	Fan+06
SDSS J113717.73+354956.9	6.0100	Fan+06
5 < z < 6		
ULAS J0148+0600	5.98	
SDSS J1411+1217	5.9270	Fan+06
SDSS J133550.80+353315.8	5.9012	Fan+06
SDSS J0005-0006	5.85	Fan+06
SDSS J0840+5624	5.8441	Fan+06
SDSS J143611.74+500706.9	5.8300	Fan+06
SDSS J104433.04-012502.2	5.7824	Fan+06
SDSS J0836+0054	5.774	Fan+06
SDSS J092721.82+200123.7	5.7722	Fan+06
SDSS J0203+0012	5.72	
SDSS J02310728	5.42	
SDSS J1659+2709	5.32	
SDSS J1208+0010	5.27	
SDSS J0915+4244	5.20	
SDSS J12040021	5.09	
4 < z < 5		
SDSS J00400915	4.98	
SDSS J0011+1446	4.95	
SDSS J22250014	4.89	
SDSS J1616+0501	4.88	
BR 12020725	4.70	
SDSS J21470838	4.60	
BR 03533820	4.59	
BR 10330327	4.52	
BR 00066208	4.52	
BR 07146449	4.49	
BR 04185723	4.48	
z < 3 − 4		
see BOSS Lyα survey		Kee-Gee?+

While the high resolution and high S/N spectroscopy is always desirable whenever available, there are a couple of ways to characterise the absorbing systems with the equivalent width and redshift using intermediate resolution spectroscopy (Rauch 1998). We explore the pixel optical depth method, EW-redshift indentification, and voigt profile decomposition to characterise the CGM/IGM environment using the synthetic spectra from simulations in the subsequent section.
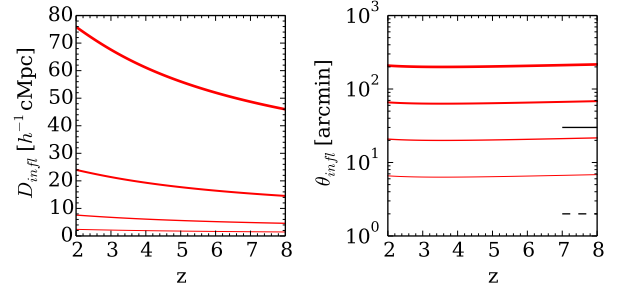
Figure 1. The comoving region of influence (left pannel) and the angular size on the sky (right pannel) for the strong absorbers with column density $N_{\rm HI} = 10^{19}, 10^{20}, 10^{21}, 10^{22} {\rm cm}^2$ (from bottom to top). The field-of-views of the Subaru/Magellan-like ground-based telescope (30arcmin, solid) and HST-like space-based telescope (2arcmin, dashed) are shown as horizontal black lines.

2.2 Galaxy fields

2.2.1 Angular coverage

The angular coverage of a survey should be large enough that the region Lyα RT influence is well included. $\theta_{\rm infl} = D_{\rm infl}/D_A(z)$ where D_A is the angular diameter distance. This requirement is easily met for most of telescope with a single field-of-view (FoV), e.g. for Subaru/Supreme-Cam $34' \times 27'$ FoV.

The region of influence can extend as large as $\sim 50h^{-1}{\rm cMpc}$ for DLAs, whereas it is as small as $\sim 2h^{-1}{\rm cMpc}$ for LLS. Since the angular size of the region of influence (ca. 10-100arcmin) stays approximately constant, the same mosaicing can be applied to survey the wide range of redshift. For the Subaru/Magellan-like ground-based telescope, the region of influence of LLSs can be covered by the single field of view. For DLA, the several mosaicing, say 2-7 tiles for one direction, is required. For the HST-like space-based telescope, also for JWST, order of 10 tiles for LLS and of 100 tiles for DLA are required.

Note that the estimate of the region of influence presented here only includes the Hubble flow. The systematic deviation due to peculiar velocity by the large-scale structure formation produces inflow. In the presence of large-scale inflow, the comoving region of influence will become larger.

2.2.2 Spectroscopic requirement

The redshift error of objects (Lyα forests and galaxies) should be below the inflow or outflow velocity scale that we want to probe. For $z = 2 − 3$ LBGs, Steidel et al. (2010) observed using metal lines that the large-scale galactic outflow spans over 100km/s-600km/s. To gain the velocity space error below 100km/s, the required absolute redshift error should be below $\Delta z = \delta v/c = 0.0003$. In terms of spectroscopy, the spectral resolution should exceed $R = \lambda/\Delta\lambda = (1+z)/\Delta z \approx 3000(1+z)$.

Table 2. Telescopes and intruments for redshift surveys with Lyα forests

Telescope/Instrument	Field of View [arcmin×arcmin]	Pixel resolution [arcsec/pixel]	Ref.
Imaging			
Subaru/Supreme-Cam	$34' \times 27'$	0.202	Ouchi+2008 ++
HST/WFC3(ACS)	$\sim 2.1'()$	0.128	Ellis+2012 (HUDF12)
Magellan/IMACS	$27.2' \times 27.2'$	0.2	Dressler+2014
Spectroscopy			
Keck/HIRES			
Keck/DEIMOS			
VLT/X-Shooter			
Gemini/GMOS			

2.2.3 Number counts of LAE/LBG selections

We estimate the expected number counts of Lyα/UV-selected galaxies in the QSO field within the field-of-view to cover the region of influence. The required flux limit provide the feasiblity of such survey strategy.

The expected number of galaxies within the survey volume is

$$N(> F_{lim}) = \Omega_{survey} \int_{z_1}^{z_2} dz \frac{d^2V}{dzd\Omega} \int_{4\pi D_L^2(z)F_{lim}}^{\infty} \frac{dn(> L, z)}{dL} dL$$

(1)

where $\frac{d^2V}{dzd\Omega} = \left|\frac{dr}{dz}\right| D_A^2(z)$ and we have assume plane-parallel approximation and $\bar{z}$ is the mean redshift depth of the survey. $z_1 = z_Q - \Delta z$ and $z_2 = z_Q$. Since the obseravtion showed that for $z = 3 - 6$ the LAE luminosity function evolves very slowly, for Schecter fit $\phi(L)dL = \phi_*(L/L_*)^\alpha e^{-L/L_*} dL/L_*$,

$$N(> F_{lim}) \approx \Omega_{survey} \int_{z_1}^{z_2} \frac{cD_A^2(z)dz}{H(z)} \phi_* \Gamma\left(1 + \alpha, \frac{4\pi D_L^2(z)F_{lim}}{L_*}\right)$$

(2)

where $\Gamma(a, x)$ is the upper incomplete Gamma function.

2.2.4 Galaxy-absorber pair counts

To measure the galaxy-absorber correlation function, we need to sample the sufficient number of the galaxy-absorber pairs to lower the random sampling error. For the simple case of Poisson error estimate, the random uncertainty in the correlation function is $\frac{\Delta\xi(r)}{1+\xi(r)} = 1/\sqrt{N_{pair}(r)}$, which is the lower bound of more realistic error (Peacock 1998). To measure the correlation function below 10% error, more than 100 pairs per bin are required. The expected number of galaxies centred at each absorber $(N_{a,pair}(r) = N_{pair}(r)/\mathcal{N})$ is $N_{a,pair}(r) = N(> F_{lim}) \int_{r-\frac{1}{2}\Delta r}^{r+\frac{1}{2}\Delta r} p(r)dr$ where $p(r)dr$ is the probability that a galaxy is found in the interval r and $r+dr$ around an absorber. For the Poisson distribution of galaxies, $p(r)dr = 4\pi r^2 dr/V_{survey}(\bar{z})$. If one expects some degree of clustering around an absorber, the probability is modifed as $p(r)dr = 4\pi r^2(1 + \xi^{expt}(r)dr/V_{survey}(\bar{z})$ where $\xi_{ag}^{expt}(r)$ is the expected absorber-galaxy correlation function. Thus, the total number of galaxy-absorber pairs for each bin Δr for each QSO field is given by $N_{pair}(r) = \mathcal{N}N_{a,pair}$,

$$N_{pair}(r) = \mathcal{N}\frac{N(> F_{lim})}{V_{survey}(\bar{z})} \int_{r-\frac{1}{2}\Delta r}^{r+\frac{1}{2}\Delta r} 4\pi r^2 \left(1 + \xi_{ag}^{expt}(r)\right) dr.$$

(3)

The linear theory expectation of galaxy-absorber correlation function is $\xi_{ag}^{lin}(r) = b_a b_g \int \Delta^2(k) \frac{\sin kr}{kr} dk (check!)$ where b_a
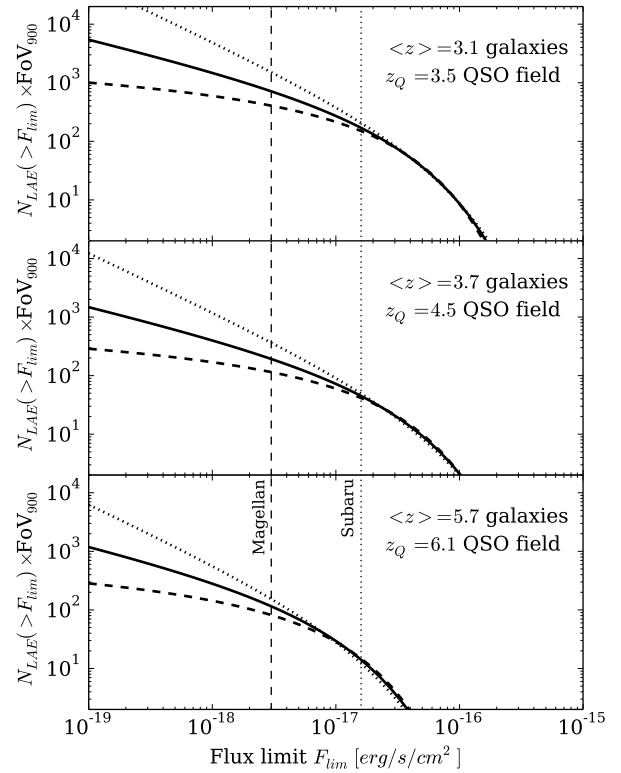

Figure 2. The expected number counts of LAEs in redshift galaxy survey in candidate QSO fields for $3 < z < 7$. y-axis shows the LAE number counts in a $30 \times 30 \text{arcmin}^2$ field-of-view $\text{FoV}_{900} = (\text{FoV}/900\text{arcmin}^2)$. The vertical lines show the practical flux limit for current survey using Subaru/Supreme-Cam (dotted; Ouchi+2008) and Magellan/IMACS (dashed; Dressler+2014). The LAE luminosity function is taken from the best-fit Schecter function of Ouchi+(2008) with three fixed faint-end slope, $\alpha = -1.0, 1.5, 2.0$ (dashed, solid, dotted lines). We assumed the entire Lyα forest region between Lyα and Lyβ lines is covered by the survey.

and b_g are the linear bias of absorbers and galaxies respectively. For $2 < z < 3$ BOSS, b_{LyF}, b_{DLA}. b_{LAE} b_{LBG}. The expected number of absorbers for each QSO spectrum is

$$\mathcal{N}(N_{\text{HI}}) = \int_{z_1}^{z_2} dz \int_{N_{\text{HI}}^{min}}^{N_{\text{HI}}^{max}} dN_{\text{HI}} \frac{d^2\mathcal{N}}{dN_{\text{HI}}dz}$$
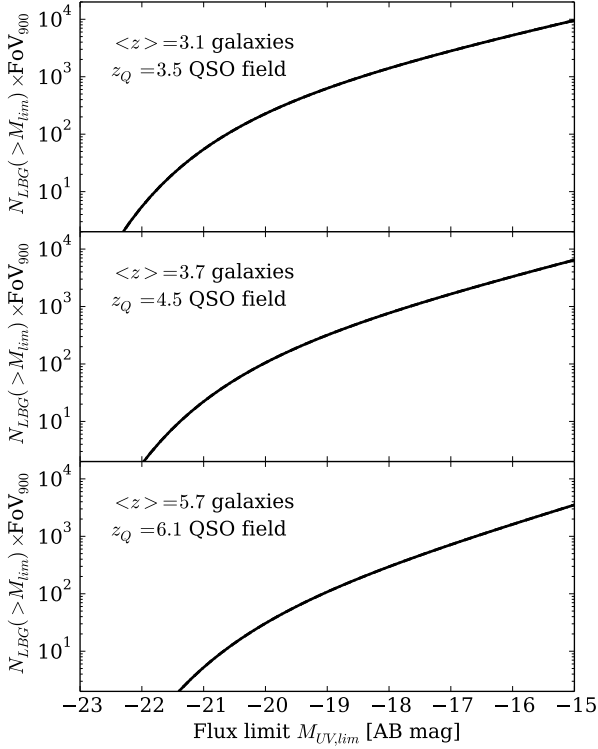
(4)

Figure 3. The expected number counts of LBGs in redshift galaxy survey in candidate QSO fields for $3 < z < 7$. y-axis shows the LBG number counts in a $30 \times 30 \text{arcmin}^2$ field-of-view $\text{FoV}_{900} = (\text{FoV}/900\text{arcmin}^2)$. The LBG UV luminosity function is taken from the best-fit Schecter function of Bouwens+(2014). We assumed the entire Lyα forest region between Lyα and Lyβ lines is covered by the survey.

(**Npair vs r for each F_{lim} case for Poisson and linear theory expectation**).

Number of QSO fields needed.

3   THEORY: OVERVIEW

Our goal is to connect the statistical formulations of the redshift-space anisotropy of galaxy-absorber systems and the cosmological Lyα radiative transfer. The formalism for the redshift-space distortion largely follows that by Fisher+1994 and Beth&White 2011. We first present the overview of our modelling framework, which is quite general treatment of the problem. In next section we model the details.

3.1   Galaxy-absorber system

The dynamics of galaxy-absorber system and the real-space clustering form the basis of joint statistical formulation of redshift-space anisotorpy and Lyα RT. The full dynamical discription of the galaxy-absorber pairs is provided by the phase-space information. The phase space distribution function of a pair is $f(v_{12}, r_{12})$ where v_{12} is the pairwise relative
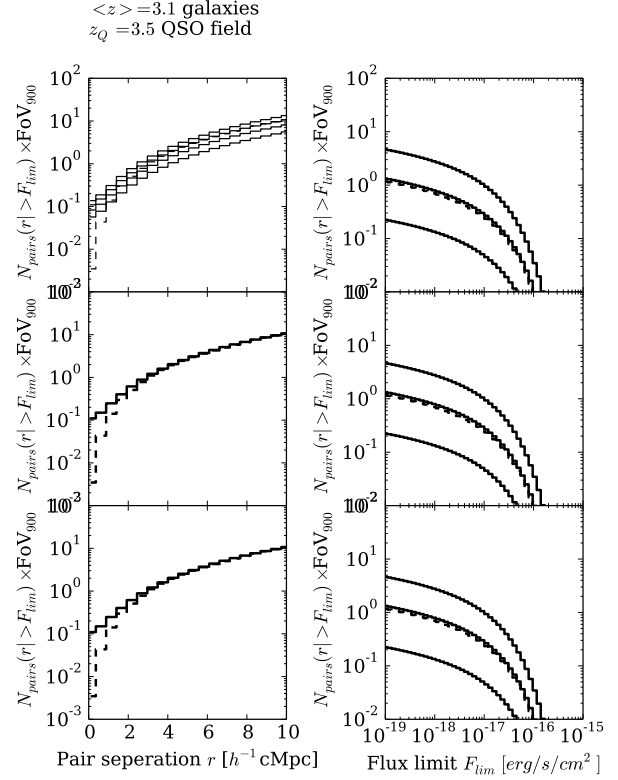

Figure 4. LAE pair counts. Need to redo this. plot something like this

velocity between galaxy and absorber and r_{12} is the galaxy-absorber comoving distance. Because of statistical isotropy and homogeneity, it only depends on the magnitude of pair-wise velocity and comoving seperation.

The real-space correlation function $\bar{n}^2 \xi(r) = f(r) = \int f(v, r) dv$??. The conditional pairwise velocity distribution function $f(v_{12}|r_{12})$ at the fixed comoving seperation r_{12} is followed from the Bayes' theorem $f(v_{12}, r_{12}) = f(v_{12}|r_{12})f(r_{12})$. The mean pairwise velocity is given by the first moment, $\langle v_{12}(r) \rangle = \int v_{12} f(v_{12}|r) dv_{12}$.

The pairwise velocity statistics is the central quantity in our formulation.

3.2   Redshift-space distortion

The redshift-space distortion is the result of the line-of-sight pecular velocity between the tracers. For our interest, the tracers are galaxies (LAEs and LBGs) and absorbers (Lyα forests and LLS/DLAs). The pairwise velocity between galaxies and absorbers imprint the redshift space distortion signature. Turner? Rudie+? have measured the redshift space distortion consistent with coherent cosmological inflow for LBG samples.

The mapping between redshift space and real space is

$$s_\perp = r_\perp, \quad s_\parallel = r_\parallel - v_{12,\parallel}/H, \quad (5)$$

The redshift-space correlation function $\xi_s(s_\parallel, s_\perp)$ can be modelled by the integration of real-space correlation function $\xi(r)$ with the pairwise velocity distribution function $f(v_{12,\parallel}|r)$ along a line-of-sight (Peeble 1980; Reid&White

(2006?); Fisher 1994-6?),

$$1+\xi_s(s_\|,s_\perp) = \int dv_{12,\|} f(v_{12,\|}|r) \left[1 + \xi(\sqrt{s_\perp^2 + (s_\| + v_{12,\|}/H)^2})\right] \quad (6)$$

This is often referred to as streaming model (Peebles 1980; Jing+).

The central ingredient of the streaming model is the pairwise velocity distribution $f(v_{12,\|}|r)$. Fisher (1995) has shown that the streaming model with linear theory for $f(v_{12,\|}|r)$ is equivalent to the familar Kaiser effect. Scoccimaro (2004) has shown that if pairwise velocity PDF is correct the streaming is valid for all scale (check the argument).

3.3 Cosmological Lyα radiative transfer

The statitical formulation of the Lyα raditive transfer can start with Paresce, McKee Bowyer 1980. The critical difference between continuum RT and line RT is that the former is sentitive to the clustering in real space whereas the latter is to in *velocity space*. The probability of an absorbering cloud's velocity within v and $v+dv$ is $p(v)dv$. Then the probability that a line-of-sight of Lyα galaxy to the observer does not coincide is $[1-p(v)]dv$. The fraction of photons absorbed is $p(v)e^{-\tau(v)}dv$

$$\langle I(v + \Delta v)\rangle = \langle I(v)\rangle \left\{(1 - p(v))\Delta v + p(v)e^{-\tau(v)}\Delta v\right\} \quad (7)$$

Forming the differential equation by $d\langle I\rangle/dv \approx \langle I\rangle[p(v)(1-e^{-\tau(v)})]$, whose solution is $\langle I\rangle = \langle I\rangle_0 e^{-\tau_{\rm eff}}$

$$\tau_{\rm eff} = \int_{-\infty}^{\infty} p(v_{12}) \left[1 - e^{-\tau(v_{12})}\right] dv_{12} \quad (8)$$

where v_{12} is the pairwise velocity of absorber and galaxy.

The pairwise velocity PDF $p(v_{12})$. Maybe an approach is cumulant expansion with respect to N-point correlation function derived from BBGKY hierarchy. The truncate with 2PCF (see Scherrer & Bertschinger 1991)? From the Bayes' rule

$$p(v_{12}) = \int p(v_{12}|r)p(r)dr \quad (9)$$

where $p(r)dr = \frac{4\pi r^2}{V}(1 + \xi(r))dr$ is the PDF from the real-space clustering of absorber around galaxy.

The end result for Gaussian pairwise velocity PDF.

$$\tau_{\rm eff} = \int dN_{\rm HI} \frac{d\mathcal{N}}{dN_{\rm HI}} \int dv p(v_{12}) \left[1 - e^{-\tau(v_{12}, N_{\rm HI})}\right] \quad (10)$$

$$p(v_{12}) = \int \frac{d^3r}{\sqrt{2\pi\sigma_{12}^2(\boldsymbol{r})}} (1 + \xi(\boldsymbol{r})) \exp\left[\frac{(v_{12} - \langle v_{12}(\boldsymbol{r})\rangle)^2}{2\sigma_{12}^2(\boldsymbol{r})}\right] \quad (11)$$

Pairwise velocity at $\boldsymbol{r}$ is $v_{12}(\boldsymbol{r})$. $\xi_v(\boldsymbol{r}) = \langle v_{12}(\boldsymbol{x})v_{12}(\boldsymbol{x}+\boldsymbol{r})\rangle$

We can imagine two models, dirac delta PDF $p(v_{12}|r) = \delta_D(v_{12} - aHr)$
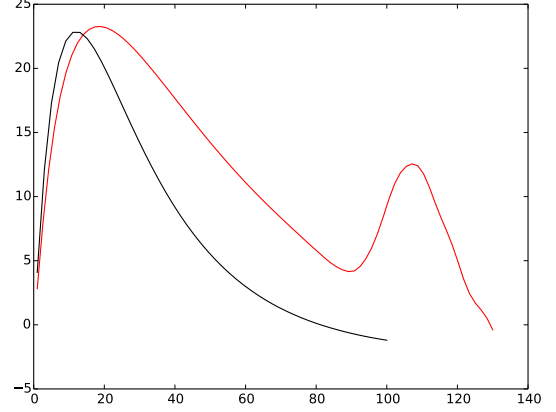
Figure 5. example, 2PCF z=0.55 compared with CLPT of M. White... Not right...

4 THEORY: GALAXY-ABSORBER REDSHIFT-SPACE ANISOTROPY

The real-space correlation function of galaxy-absorber system in the linear theory is

$$\xi(r) = b_a b_g \int_0^\infty \Delta_L^2(k) j_0(kr) \frac{dk}{k} \quad (12)$$

where $j_0(kr)$ is the 0th spherical Bessel function of the first kind.

4.1 Redshift-space correlation function

Our aim is to develop a theory to interpret the observation of the galaxy-absorber correlation function in the redshift space. The redshit-space correlation function $\xi(s_\|, s_\perp)$ shows the anisotropy due to the redshift-space distortion imprinted by the peculiar velocity field. Although we do not intend to use such observations to measure $f = d\ln D/d\ln a$ as in modern LLS survey (e.g. BOSS, WiggleZ), we start with the linear theory to build up a solid understanding.

The two-dimensional correlation function is usually expanded in Legendre Polynomials $L_\ell(\mu_s)$ where $\mu_s = s_\|/s$ (Reid&White, Reid+2012; Hamilton 1992),

$$\xi(s, \mu_s) = \sum_{\ell=0}^{\infty} \xi_\ell(s) L_\ell(\mu_s), \quad (13)$$

where

$$\xi_\ell(s) = \frac{2\ell + 1}{2} \int d\mu_s \xi(s, \mu_s) L_\ell(\mu_s). \quad (14)$$

For large-scale structure studies, the first three even Legendre moments $\xi_0(s)$, $\xi_2(s)$ and $\xi_4(s)$ are usually considered. The quadrupole-monopole ratio ξ_2/ξ_0 is positive for streching in radial direction and negative for flattening. Coherent inflow produce the negative quadrupole-monopole ratio, while random velocity dispersion and coherent outflow give positive value.

In linear theory, Kaiser formula translates to (Hamilton 1992; Reid&White 2011)

$$\xi_\ell(s) = i^\ell \int \frac{dk}{k} \Delta_\ell^2(k) j_\ell(ks), \quad (15)$$

where

$$\Delta_0^2(k) = \Delta_L^2(k)(b^2 + \frac{2}{3}bf + \frac{1}{5}f^2), \qquad (16)$$

$$\Delta_2^2(k) = \Delta_L^2(k)(\frac{4}{3}bf + \frac{4}{7}f^2), \qquad (17)$$

$$\Delta_4^2(k) = \Delta_L^2(k)(\frac{8}{35}f^2), \qquad (18)$$

4.1.1 Pairwise velocity PDF

For the perfectly coherent velocity field,

$$1+\xi^s(s_\parallel, s_\perp) = \int dr_\parallel \left[1 + \xi(\sqrt{s_\perp^2 + r_\parallel^2})\right] \delta_D \left[s_\parallel - r_\parallel - \mu v_{12}(r)\right] \qquad (19)$$

where $r = \sqrt{r_\perp^2 + r_\parallel^2}$ and $\mu = r_\parallel/r$. The redshift-space correlation function is then given by $\xi^s(s_\parallel, s_\perp) = \xi(\sqrt{s_\perp^2 + r_\parallel^2(s_\parallel)})$ where $r_\parallel(s_\parallel)$ is the solution of implicit equation $s_\parallel = r_\parallel \left(1 - \frac{v_{12}(r)}{r}\right)$.

By assuming the velocity PDF is gaussian, we arrive at the Gaussian streaming model (Reid&White 2011)

$$1 + \xi^s(s_\parallel, s_\perp) = \int \frac{dy}{\sqrt{2\pi\sigma_{12}^2(r,\mu)}} \times \qquad (20)$$
$$\left[1 + \xi(\sqrt{s_\parallel^2 + y^2})\right] \exp\left[-\frac{(s_\parallel - y - \mu v_{12}(r))^2}{2\sigma_{12}^2(r,\mu)}\right]$$

4.2 Pairwise velocity statistics and BBGKY hierarchy

The streaming models require the modelling of the pairwise velocity statistics; mean pairwise velocity $v_{12}(r)$ and pairwise velocity dispersion $\sigma_{12}^2(r,\mu)$. The BBGKY hierarchy provides a framework to relate the pairwise velocity statistics to the real-space clustering (Davis&Peebles 1977; Peebles 1980; Fry+; Hamilton 1988). Formally, the BBGKY hierarchy provides the relation between velocity statistics such as pairwise streaming velocity and velocity dispersion and N-point correlation function. We cast the traditional BBGKY hierarchy expressed in terms of dark matter or galaxies in the application to galaxy-absorber systems. The absorbers are the result of the IGM fluctuation in the cosmic web environment. We approximate the absorbers as a cloud. However in reality, Lyα forest or self-shielded system, LLS/DLA, should be viewed in terms of cosmic web. We mitigate this by considering the filaments or walls of cosmic web as connection of clouds in a appropriate geometry.

Suppose Phase-space of galaxy and absorbers **do this with Kilmontovich formalism and get BBGKY hierarchy and pair conservation laws.** The first velocity moment of the BBGKY hierarchy expresses the the conservation of pairs. This can more easily derived from the conservation argument (Peebles 1976?; White's book). Suppose particles (galaxy-absorber pair) within a comoving radius $< r$ centred at a particle, $N(<r,t) = \bar{n}(0)\int_0^r 4\pi r'^2 dr'(1+\xi(r,t))$ where $\bar{n}(0)$ is the mean comoving number density (constant over redshift) and $\xi(r,t)$ is the particle-particle (galaxy-absorber) correlation function. The change in the total particle number $N(<r,t)$ is determined by the flux through the surface of sphere of radius r, which is $4\pi r^2 \bar{n}(0)(1 +$
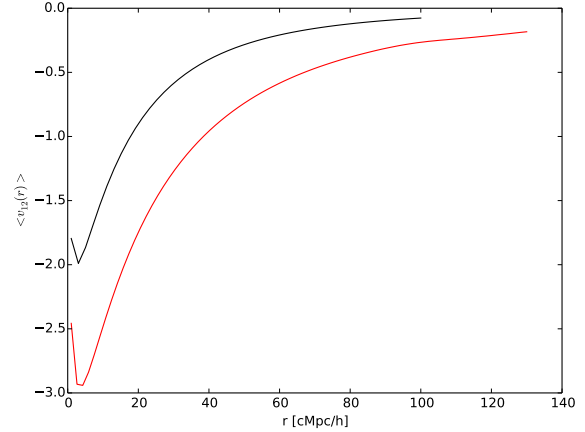

Figure 6. Pairwise velocity field. redo this

$\xi(r,t))\langle v_{12}\rangle$. Note that $\langle v_{12}\rangle$ is the mean pairwise *comoving* velocity. [1] We adopt the convention that the pairwise velocity is negative for inflow and positive for outflow.

Thus, when the total number of particles are conserved,

$$\frac{\partial N}{\partial t} + 4\pi r^2 \bar{n}(0)(1 + \xi(r,t))\langle v_{12}\rangle = 0 \qquad (23)$$

By rearranging for $\langle v_{12}\rangle$, this follows the mean pairwise velocity field as (Davis&Peebles 1977; Cooray & Sheth 2002; White)

$$\langle v_{12}(r,t)\rangle = -\frac{1}{1+\xi(r,t)}\frac{1}{r^2}\frac{\partial}{\partial t}\int_0^r \xi(r',t)r'^2 dr' \qquad (24)$$

For linear theory, the correlation function scales as $\propto D(t)^2$, the pairwise velocity field for unbiased tracer from the linear theory.

$$v_{12}(r) = -\frac{Hf(\Omega_m)}{\pi^2}\int P_L(k)j_1(kr)kdk \qquad (25)$$

where $f(\Omega) = d\ln D/d\ln a$.

For self-similar clustering,...

4.2.1 Lagrangian formulation

The linear theory and the self-similar clustering hypothesis provides the prototype of real-space 2PCF evolution. The pair conservation law is more general, which can be applied to outflow. We employ the Lagrangian picture to illustrate the evolution of 2PCF (Matsubara 2008, Carlson+; White 2014).

Lagrangian displacement field $\boldsymbol{\Psi}$ for a fluid element at $\boldsymbol{q}$ at some initial time,

$$\boldsymbol{r} = \boldsymbol{q} + \boldsymbol{\Psi}(\boldsymbol{q},t) \qquad (26)$$

---

[1] To avoid a confusion in various form appear in the literature, proper velocity is $\langle v_{12}^{proper}\rangle = a\langle v_{12}^{comoving}\rangle$.

$$\frac{\langle v_{12}^{proper}(r,a)\rangle}{Har} = -\frac{1}{1+\xi(r,a)}\frac{a}{r^3}\frac{\partial}{\partial a}\int_0^r \xi(r',a)r'^2 dr' \qquad (21)$$

in the proper coordinates??,

$$\frac{\partial \xi}{\partial t} + \frac{1}{r^2}\frac{\partial}{\partial r}\left[r^2(1+\xi)\langle v_{12}(r,a)\rangle\right] = 0 \qquad (22)$$

The mass conservation implies

$$1 + \delta(\boldsymbol{r}) = \int d^3q [1 + \delta(\boldsymbol{q})] \delta_D[\boldsymbol{r} - \boldsymbol{q} - \boldsymbol{\Psi}(\boldsymbol{q}, t)] \qquad (27)$$

5 THEORY: THE ENVIRONMENTAL DEPENDENCE OF Lyα VISIBILITY

5.1 The region of influence

For both EoR $z > 6$ (McQuinn+; Dikjstra+) and the post-reionized universe $2 < z < 6$ (Zheng+; Dijkstra&Wyithe), the IGM environment influence the visibility of Lyα-emitting galaxies. The degree of the impact depends on the amount of clustering of gas, velocity field, and photoionization background in the vicinity of the galaxies. The Lyα radiative transfer is sensitive to the velocity structure. The gas velocity field is nonlinear in and out of galactic haloes, but at large enough distance it would converge to Hubble flow. The region of influence of Lyα RT is most directly characterized in the velocity space. The wing approximation to the Lorentz profile $\varphi_\nu = \frac{\Lambda/4\pi^2}{(\nu-\nu_\alpha)^2 + (\Lambda/4\pi^2)^2} \approx \frac{\Lambda}{4\pi^2(\nu-\nu_\alpha)^2}$ where $\Lambda = 6.25 \times 10^8 s^{-1}$ is the damping coefficient. The optical depth of an absorber of column density $N_{\rm HI}$ and total (hubble flow plus peculiar) proper velocity v_c is $\tau_\alpha(\nu_e) = \sigma_\alpha N_{\rm HI} \varphi_\nu[\nu_e(1 - v_c/c)]$ The absorber velocity that gives the optical depth τ_α against Lyα line emission from galaxies is

$$v_c(\tau_\alpha) = c\sqrt{\frac{\sigma_\alpha N_{\rm HI} \Lambda}{4\pi^2 \nu_\alpha^2 \tau_\alpha}} = 507.3 \tau_\alpha^{-1/2} \left(\frac{N_{\rm HI}}{10^{20} cm^2}\right)^{1/2} \rm km/s \qquad (28)$$

For a strong absorbing cloud to give the optical depth of unity (37% transmission) against the Lyα line emission, the absorbing cloud cannot be outflowing relative to the central galaxy more than $\sim 500 - 2800$km/s. This defines the region of influence of Lyα RT in the velocity space. To translate the region of influence to the real space we need to know the velocity field around a galaxy. For pure Hubble flow the comoving region of influence is

$$D_{\rm infl} = \frac{v_c(\tau_\alpha)}{H_0} \frac{1+z}{[\Omega_m(1+z)^3 + \Omega_\Lambda]^{1/2}} \qquad (29)$$

5.2 Statistical formulation

The statitical formulation of the Lyα raditive transfer can start with Paresce, McKee Bowyer 1980. An alternative derivation, which clarifies the implicit assumptions and allow generalization, is shown in Appendix. The critical difference between continuum RT and line RT is that the former is sentitive to the clustering in real space whereas the latter is to in *velocity space*. The probability of an absorbering cloud's velocity within v and $v + dv$ is $p(v)dv$. Then the probability that a line-of-sight of Lyα galaxy to the observer does not coincide is $1 - p(v)dv$. The fraction of photons absorbed is $p(v)e^{-\tau(v)}dv$

$$\langle I(v+\Delta v)\rangle = \langle I(v)\rangle \left\{(1 - p(v)\Delta v) + p(v)e^{-\tau(v)}\Delta v\right\} \qquad (30)$$

Forming the differential equation by $d\langle I\rangle/dv \approx \langle I\rangle[p(v)(1 - e^{-\tau(v)})]$, whose solution is $\langle I\rangle = \langle I\rangle_0 e^{-\tau_{\rm eff}}$

$$\tau_{\rm eff} = \int_{-\infty}^{\infty} p(v_{12}) \left[1 - e^{-\tau(v_{12})}\right] dv_{12} \qquad (31)$$

where $v_{12}^{tot} = aHr_{12} + v_{12}$ is the *total, proper pairwise velocity* of absorber and galaxy. By transforming the variables r_{12}, v_{12} into v_{12}^{tot},

$$
\begin{aligned}
f(v_{12}^{tot}) &= \iint \delta_D \left[v_{12}^{tot} - (Hr_{12} + v_{12})\right] f(v_{12}, r_{12}) dv_{12} dr_{12} \\
&= \int f(v_{12}^{tot} - Hr_{12}|r_{12}) f(r_{12}) dr_{12} \qquad (32)
\end{aligned}
$$

where $f(r)dr = \frac{4\pi r^2}{V}(1 + \xi(r)) dr (NO!)$ CORRECT ONE is $f(r)dr = \frac{1}{L}(1 + \xi(r)) dr$ (pre-factor dendendence is geometric factor for 1D along a skewer it does not enter!) is the PDF from the real-space clustering of absorber around galaxy.

total velocity $v_\parallel^{tot} = Hs_\parallel = H(r_\parallel + v_\parallel/H)$

$$I(s + ds) = I(s) \left\{1 - p(s_\parallel, N_{\rm HI}) ds_\parallel + p(s_\parallel, N_{\rm HI}) e^{-\tau(s_\parallel, N_{\rm HI})} ds\right\} \qquad (33)$$

The end result for Gaussian pairwise velocity PDF.

$$\tau_{\rm eff} = \int dN_{\rm HI} \frac{\partial^2 \mathcal{N}}{\partial N_{\rm HI} \partial z} \left|\frac{dz}{dr}\right| \int dv f(v_{12}) \left[1 - e^{-\tau(v_{12}, N_{\rm HI})}\right] \qquad (34)$$

$$f(v_{12}) = \int \frac{dr}{\sqrt{2\pi\sigma_{12}^2(r)}} (1 + \xi(r)) \exp\left[\frac{(v_{12}^{tot} - Hr - \langle v_{12}(r)\rangle)^2}{2\sigma_{12}^2(r)}\right] \qquad (35)$$

The end result for Gaussian pairwise velocity PDF.

$$\tau_{\rm eff} = \int dN_{\rm HI} \frac{d\mathcal{N}}{dN_{\rm HI}} \int dv f(v_{12}) \left[1 - e^{-\tau(v_{12}, N_{\rm HI})}\right] \qquad (36)$$

$$f(v_{12}) = \int \frac{4\pi r^2 dr}{\sqrt{2\pi\sigma_{12}^2(r)}V} (1 + \xi(r)) \exp\left[\frac{(v_{12}^{tot} - Hr - \langle v_{12}(r)\rangle)^2}{2\sigma_{12}^2(r)}\right] \qquad (37)$$

The end result for Gaussian pairwise velocity PDF.

$$\tau_{\rm eff} = \int dN_{\rm HI} \frac{d\mathcal{N}}{dN_{\rm HI}} \int dv f(v_{12}) \left[1 - e^{-\tau(v_{12}, N_{\rm HI})}\right] \qquad (38)$$

$$f(v_{12}) = \int \frac{4\pi r^2 dr}{\sqrt{2\pi\sigma_{12}^2(r)}V} (1 + \xi(r)) \exp\left[\frac{(v_{12}^{tot} - Hr - \langle v_{12}(r)\rangle)^2}{2\sigma_{12}^2(r)}\right] \qquad (39)$$

For generalization to the anisotropic real-space clustering, e.g. biconical outflow + two cold streaming model

$$f(v_{12}) = \int \frac{d^3r}{\sqrt{2\pi\sigma_{12}^2(\boldsymbol{r})}} (1 + \xi(\boldsymbol{r})) \exp\left[\frac{(v_{12} - \langle v_{12}(\boldsymbol{r})\rangle)^2}{2\sigma_{12}^2(\boldsymbol{r})}\right] \qquad (40)$$

Pairwise velocity at $\boldsymbol{r}$ is $v_{12}(\boldsymbol{r})$. $\xi_v(\boldsymbol{r}) = \langle v_{12}(\boldsymbol{x}) v_{12}(\boldsymbol{x} + \boldsymbol{r})\rangle$

We can imagine two models, dirac delta PDF $p(v_{12}|r) = \delta_D(v_{12} - aHr)$

5.3 Caveats

5.3.1 Pairwise velocity PDF

How good is the gaussian approximation to pairwise velocity PDF? The assumption that the pairwise velocity PDF may introduce systematic bias in analytic model. Scoccimaro 2004 has studied that the pairwise velocity PDF is in fact highly non-gaussian with skewness and kurtosis. Tinker 2005? modelled the non-gaussian pairwise velocity PDF in

the HOD framework. Generalisation can also be done possibly by the cumulant expansion or Edgeworth expansion (e.g. Matsubara2008+; Sherrer&Bertschinger 1991).

Scoccimaro 2004 argued that the direct recontruction of the PDF from redshift-space clustering measurement is in general impossible, which must rely on the assumption of scale-independent PDF or Gaussianity.

The pairwise velocity PDF $p(v_{12})$. Maybe an approach is cumulant expansion with respect to N-point correlation function derived from BBGKY hierarchy. The truncate with 2PCF (see Scherrer & Bertschinger 1991)?

6   SIMULATION

6.1   Cosmological hydrodynamical simulation of the IGM

We carried out the cosmological hydrodynamical simulation of the IGM using AMR hydro/N-body code RAMSES (Teyssier 2002). We performed a series of adiabatic simulation with varying box size and resolution elements for convergence test.

We adopt the quasi-Lagrangian refinement strategy with refinement criterion of 10 particles by which the cell is refined when the number of dark matter particle or equivalent gas mass exceeds 10.

The initial condition is generated with COSMICS package (Bertschinger 1996?). The COSMICS package is initialized by setting the initial rms fluctuation $\sigma_8(z = z_{ini}) = 0.03$. Because the resolution of simulations are varying the initial redshift is elevated to lower redshift for lower resolution simulation. The initial temperature is set as $T = 650$K. This is compromise because the adiabatic simulation does not include Compton heating from CMB and cooling. The IGM only be cooled or heated by adiabatic process.

The haloes are identified by HOP algorithm (Eisenstein+; Aubert).

6.2   Radiative transfer

We introduce the self-shielded gas by Rhamati+ criterion. The method is calibrated based on radiative transfer simulation.

6.3   Synthetic QSO spectra

6.4   Synthetic galaxy catalogue

7   COMPARISON BETWEEN MODEL AND SIMULATION

7.1   unbiased tracer: gas and dark matter

8   SURVEY: MOCK

ACKNOWLEDGMENTS

Some of the calculations in this paper is computed using python mpmath library (Johansson et al. 2010).

REFERENCES

Johansson F., et al., 2010, mpmath: a Python library for arbitrary-precision floating-point arithmetic (version 0.14)
Rauch M., 1998, ARA&A, 36, 267
Rudie G. C., Steidel C. C., Trainor R. F., Rakic O., Bogosavljević M., Pettini M., Reddy N., Shapley A. E., Erb D. K., Law D. R., 2012, ApJ, 750, 67
Steidel C. C., Erb D. K., Shapley A. E., Pettini M., Reddy N., Bogosavljević M., Rudie G. C., Rakic O., 2010, ApJ, 717, 289

APPENDIX A: STATISTICAL FORMULATION OF RADIATIVE TRANSFER

We present the statistical formulation of radiative transfer, which is the application and the substantial generalization of the ideas appeared in Parsce+ 1980, Haardt & Madau; Zuo; Meiksin& White; Kakiichi+2012.

The cosmological radiative transfer through the IGM, neglecting the effect of re-emission and scattering along a line-of-sight is described by

$$\frac{1}{c}\frac{\partial I_\nu}{\partial t} + \boldsymbol{n}\cdot\boldsymbol{\nabla} I_\nu - \frac{H + \boldsymbol{n}\cdot\boldsymbol{\nabla}\boldsymbol{v}\cdot\boldsymbol{n}}{c}\nu\frac{\partial I_\nu}{\partial\nu} + 3\frac{H}{c}I_\nu = -\sigma_\alpha n_{HI}\varphi_\nu I_\nu \quad \text{(A1)}$$

where I_ν is the specific intensity, $\boldsymbol{v}$ is the peculiar velocity, $\boldsymbol{n}$ is the unit direction vector of rays, $\sigma_\alpha = 0.011\text{cm}^2\text{Hz}$ is the Lyα cross section, φ_ν is the line profile of Lyα resonance line. $\boldsymbol{n}\cdot\boldsymbol{\nabla}\boldsymbol{v}\cdot\boldsymbol{n}$ term is the Doppler shift effect. The solution to the cosmological radiative transfer equation is

$$I_\nu = \frac{I_\nu(z_s)}{(1+z_s)^3}e^{-\tau_\alpha(\nu_e, z_s)} \quad \text{(A2)}$$

where the optical depth τ_α is given by

$$\tau_\alpha(\nu_e, z_s) = \int_0^{z_s} dz' \left|\frac{dl_p}{dz'}\right| n_{HI}(z')\varphi_\nu\left[T(z'), \nu_e\left(\frac{1+z'}{1+z_s}\right)\left(1 - \frac{v(z')}{c}\right)\right] \quad \text{(A3)}$$

We are interested in the statistical properties of the radiation field I_ν. The probability distribution function $P(I_\nu)dI_\nu$ provides the probability that an radiating source is observed with the specific intensity I_ν. The averege specific intensity for all the sources $\langle I_\nu \rangle = \int I_\nu P(I_\nu)dI_\nu$ corresponds to stacking the observed spectra of galaxies or QSOs.

Suppose a sphere of radius R centred at the obeserver that is sufficiently large to contain the source. In the picture that the IGM consists of absorbers of column density $N_{HI,i}$ and redshift

Suppose a line-of-sight skewer of length R. The optical depth along a line-of-sight is

$$\tau(\nu_e) = \sigma_\alpha \int_0^R dr' n_{HI}(r')\varphi(r') = \sigma_\alpha \sum_{i=1}^{\mathcal{N}} N_{HI,i}\varphi(r_i)\Theta(r_i - R) \quad \text{(A4)}$$

Table 3. Simulation set up

name	Box size L [h^{-1}cMpc]	$N_{\rm DM}$	$N_{\rm grid}(base)$	$N_{\rm grid}(fine)$	$m_{\rm DM}$ [h^{-1}M$_\odot$]	$\Delta L(base)$ [h^{-1}ckpc]	$\Delta L(fine)$	z_{ini}	$J_{21}, \alpha, z_{reion}$
static grid + adiabatic									
L10P256G256R0	10	256^3	256^3		3.57×10^6	39.1		276	
L20P256G256R0	20	256^3	256^3		2.86×10^7	78.1		237	
L40P256G256R0	40	256^3	256^3		2.29×10^8	156.2		199	
L60P256G256R0	60	256^3	256^3		7.72×10^8	234.4		178	
AMR grid + adiabatic									
L40P256G256R2	40	256^3	256^3	1024^3	2.29×10^8	156.2	39.1	199	
static grid run + UV background									
L40P256G256R0	40	256^3	256^3		2.29×10^8	156.2		199	1.0, 1.0, 8.5